

Journal of Biomedical Optics

BiomedicalOptics.SPIEDigitalLibrary.org

Laser structuring of carbon nanotubes in the albumin matrix for the creation of composite biostructures

Alexander Yu. Gerasimenko
Olga E. Glukhova
Georgy V. Savostyanov
Vitaly M. Podgaetsky

SPIE.

Alexander Yu. Gerasimenko, Olga E. Glukhova, Georgy V. Savostyanov, Vitaly M. Podgaetsky, "Laser structuring of carbon nanotubes in the albumin matrix for the creation of composite biostructures," *J. Biomed. Opt.* **22**(6), 065003 (2017), doi: 10.1117/1.JBO.22.6.065003.

Laser structuring of carbon nanotubes in the albumin matrix for the creation of composite biostructures

Alexander Yu. Gerasimenko,^{a,*} Olga E. Glukhova,^b Georgy V. Savostyanov,^b and Vitaly M. Podgaetsky^a

^aNational Research University of Electronic Technology, Department of Biomedical Systems, Zelenograd, Moscow, Russia

^bSaratov National Research State University, Department of Radiotechnique and Electrodynamic, Saratov, Russia

Abstract. This paper presents the composite biostructures created by laser structuring of the single-walled carbon nanotubes (SWCNTs) in an albumin matrix. Under the exposure of femtosecond laser radiation, the heating of the albumin aqueous solution causes liquid water to evaporate. As a result, we obtained a solid-state composite in the bulk or film form. Using the molecular dynamic method, we showed the formation of a framework from SWCNTs by the example of splicing of the open end of one nanotube with the defect region of another nanotube under the action of the laser heating. Laser heating of SWCNTs up to a temperature of 80°C to 100°C causes the C—C bond formation. Raman spectra measured for the composite biostructures allowed us to describe the binding of oxygen atoms of amino acid residues of the albumin with the carbon atoms of the SWCNTs. It is found that the interaction energy of the nanotube atoms and albumin atoms amounts up to 580 kJ/mol. We used atomic force microscopy to investigate the surface of the composite biostructures. The pore size is in the range of 30 to 120 nm. It is proved that the proliferation of the fibroblasts occurred on the surface of the composite biostructures during 72 h of incubation. © 2017 Society of Photo-Optical Instrumentation Engineers (SPIE) [DOI: 10.1117/1.JBO.22.6.065003]

Keywords: laser structuring; femtosecond radiation; composite biostructure; carbon nanotubes; framework; living cells.

Paper 170172PR received Mar. 19, 2017; accepted for publication May 30, 2017; published online Jun. 20, 2017.

1 Introduction

Recently, the tissue engineering is intensively developing with the application of modern methods of laser optics. This interdisciplinary branch is an alternative to the common practice of human organ transplantation. Its aim is the regeneration of the vital functions of an organism by the replacement of pathologically impaired biological tissues, their preservation, and maintenance. Of particular importance is the search for ways to develop new synthetic implantation materials for stimulating cell proliferation during tissue formation.¹⁻⁴

There are many papers that describe how to obtain three-dimensional (3-D) composite structures using laser stereolithography, selective sintering, and polymerization of liquid and powder materials.⁵⁻¹⁰ Due to the development of femtosecond lasers, the two-photon polymerization of 3-D nano-objects became more popular.¹¹⁻¹⁴ A multiphoton absorption and local polymerization in the laser beam waist region can be achieved by means of the focused femtosecond laser beam with the wavelength corresponding to the transparency of the created composite structure. Macromolecules are formed from the initial monomer during the polymerization process. The purpose of this process is to create the active centers in a liquid reactive medium using triggering laser radiation. These centers initiate the growth of the polymer chains while interacting with the molecules of the monomer. Since the active centers appear only in the irradiated region, the polymerization proceeds mainly in this area, that is, the spatial selectivity of laser polymerization is achieved. The active centers are formed when the photopolymer interacts with the radiation of a certain spectral range. A high

quantum efficiency of laser polymerization requires less power from the triggering radiation, because the absorption of one quantum of radiation causes polymerization of up to 10⁴ molecules of monomer. The absorption coefficient must be large enough for complete absorption in a thin layer (0.05 to 0.5 mm) of the photopolymer. A film of solid polymer is formed in the irradiated region. However, using such methods, it is difficult to create large 3-D structures for the manufacturing of medical implants.

This paper presents the results of the theoretical and experimental investigations of the creation of the composite biostructures by laser structuring of the carbon nanotubes (CNTs) in the water matrix of albumin.

2 Methodology

The water-protein suspension was used as an initial medium. We have chosen the most photostable type of protein—albumin (BioClot, Germany). Albumin is widely applied for laser welding of the biological tissues as a laser solder.^{15,16} This transport protein is about 60% of the blood plasma proteins and its average concentration in plasma is ~40 g/L. Albumin has the lowest molecular weight (~69,000) among all the blood plasma proteins. The albumin transport function is the transfer of free fatty acids, cholesterol, and other biologically active substances. The secondary or tertiary conformational structure under the slight protein load of the toxins is typical for albumin. The picture of the dried drops of a freshly prepared aqueous solution of serum albumin is characterized by a large number of radial cracks that form arches on the edge of the drop. It is well studied at the atomic-level structure: the molecule of albumin has two

*Address all correspondence to: Alexander Yu. Gerasimenko, E-mail: gerasimenko@bms.zone

versions (isomers), which are a rotational ellipsoid and an irregular triangular prism.¹⁷

CNTs were used as a reinforcing filler in an albumin matrix. CNTs are allotropic forms of carbon and have a filamentary structure. CNTs have attracted attention from the researchers due to their high mechanical strength, and excellent thermal and electrical properties. The sizes of CNTs are close to the sizes of the main components of the natural cellular matrix, and their mechanical properties are similar to the properties of the protein structures.^{18–20}

To create the composite biostructures, we used single-walled carbon nanotubes (SWCNTs). Nanotubes were synthesized by an arc discharge method using Ni/Y catalyst, then they are cleaned in a mixture of HNO₃/H₂SO₄ with the following washing until neutral reaction.²¹ The average diameter of the synthesized nanotubes is 1.4 to 1.6 nm, length is 0.3 to 0.8 μm, and a specific surface is ~400 m²/g. The purity of SWCNTs is 97.16%. Figure 2(a) shows the scanning electron microscopy (SEM) image of SWCNTs.

The laser technology in the formation of the composite biostructures included several steps. The first step was the preparation of an aqueous colloidal solution of SWCNTs (dispersing medium).²² To do this, SWCNTs with the concentration of 0.1 g/L were added to pure water to research the cells. The obtained solution was subjected to the powerful ultrasonic probe homogenizer (time, 30 to 40 min; power, 40 W) in order to eliminate discontinuities associated with the conglomeration of SWCNTs in bundles. The second step was the preparation of an albumin aqueous solution with SWCNTs. The albumin powder was dissolved in an aqueous solution of SWCNTs at a concentration of 25 wt. %. Further, the composition was dispersed in an ultrasonic bath until the solution was completely homogeneous (time: 40 to 60 min). Low power ultrasound (power <10 W) was used in order to prevent the damaging of the albumin molecules structure.

A key feature of this method of forming the composite biostructures was the use of an unfocused laser beam, which was directed at the albumin aqueous solution of CNTs. The formation of solid material was caused by the evaporation of the liquids under laser irradiation.

A titanium-sapphire (Ti:Sa) femtosecond laser was used to obtain the composite biostructures based on CNTs in an albumin aqueous matrix. The laser's generation wavelength was equal to 810 nm. The pulse duration was 140 fs, and the frequency was 80 MHz. The radiation power of the laser was equal to 2 W. The reason for using a femtosecond laser is a high energy/power of pulses and a high frequency of their following (duty cycle of ~6 × 10⁵). This allows us to control the heating of the albumin

aqueous solution up to the desired temperature without destroying the 3-D structure of the albumin molecules. Nevertheless, the use of laser radiation with longer pulse duration is also possible.

Figure 1(a) is a scheme of irradiation of the albumin aqueous solution of CNTs using a laser beam. A pulsed radiation was produced by a laser (1) and passed through the Glan prism (2), which was used to vary the radiation power. Then, the radiation was divided into two parts with a beamsplitter (3). The first part of the radiation was incident upon the power detector (5) through a calibrated neutral light filter (4). The second part of the radiation was rotated 90 deg by an angle prism (6) and incident on the negative lens (7). Defocused laser radiation (8) was entered the objective lens (9) and acquired the necessary diameter (10) to influence the albumin aqueous solution of CNTs (11) in the container (12). The radiation had Gaussian spatial profile (13). The diameter of the incident beam was equal to the diameter of the container with the albumin aqueous solution of CNTs. The thickness of the solution layer was ~5 mm. The action of the laser radiation on the albumin aqueous solution was performed until the solid-state composite material was formed. The sizes and shape of the bulk composite biostructure directly depend on the shape of the container in which the albumin aqueous solution of CNTs was located. The external view of the bulk composite biostructure with a height of 8 mm and diameter of 10 mm is shown in Fig. 1(b).

To obtain a composite film sample, we performed a uniform application of the albumin aqueous solution of SWCNTs to the silicon substrate using the ultrasonic deposition method or spin coating. The thickness of the solution layer was 20 to 40 μm. Further, a laser radiation was directed to a silicon substrate with a layer of solution. The irradiation of the solution was carried out until the liquid evaporated and a solid film appeared [Fig. 1(c)]. The thickness of the composite biostructure film was in the range of 5 to 10 μm. The diameter of the film of a circular shape was 10 mm and depended on the area of the incident laser radiation.

3 Results

3.1 Creation of the Composite Biostructures

In order to investigate the formation mechanism of the composite biostructures, we performed numerical calculations using the molecular dynamics method. We simulated the formation of the framework of CNTs under laser radiation. As is known, the nanotubes contain many defects formed during their synthesis. It is predicted that the nanotubes most likely will be spliced exactly in these defective areas. Besides,

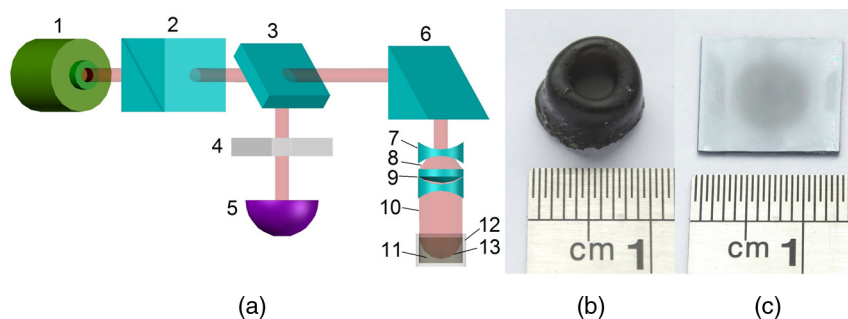


Fig. 1 (a) Scheme of the formation of the composite biostructures in (b) bulk and (c) film forms on a silicon substrate.

defective areas will heat up most noticeably under heating tubes by a laser beam, as the thermal conductivity is markedly reduced in these areas.²³

We considered two tubes with the chiral indices (22, 22) and (24, 24) as their diameters are the closest to the data yielded by the experiment—1.4 and 1.6 nm, respectively. We simulated the most common structural defects: single vacancy (1V) defect, double vacancy (2V) defect, and Stone–Wales (SW) defect.

The obtained experimental data show a high mechanical strength of the composite biostructure (hardness was ~300 MPa), indicating the formation of covalent bonds in the area of connection of the tubes. It is well known that defective areas of the tubes are chemically more active than defect-free areas.²⁴ The resulting branched structure of the nanotubes is shown in Fig. 2(b).

3.2 Simulation of the Laser Creation of Carbon Nanoframework

At an initial moment of the simulation, the nanotubes were randomly located in the periodic box in an aqueous environment. The temperature increased from 90°C to 200°C and was regulated by a Nose–Hoover thermostat. The formation of the contact between the SWCNTs was performed using open source software for molecular modeling Kvazar,²⁵ simulating the tube heating under laser radiation. The energy of the nanotubes was calculated using a reactive empirical bond order potential force field.²⁶ This approach was successfully used earlier by the authors in the predictive modeling of the structure formation of the carbon nanocomposites and other complex hybrid carbon materials.^{27,28} The simulation of the formation of C–C bonds between defect-containing nanotubes was performed within a few nanoseconds. Figure 3 shows the results of the numerical experiments. Figure 3(a) shows “the splice” of an open end of the nanotube (22, 22) with the defective area of the nanotube (24, 24). The defective area contains two 2V defects and one SW defect. Other concentrations of defects including 1V defect were also examined. The enthalpy of formation for the contact was calculated during the splicing of the SWCNTs. Figures 3(b) and 3(c) show the changes in enthalpy of formation with the numbers of chemical bonds for different defective areas. In each case, a defective area contained a different number of defects (1V, 2V, and SW). The presented enthalpy graphs allow us to conclude that the formation of the framework of SWCNT is more energetically favorable in the presence of four 1V defects in the area of the connection of the tubes.

The lengths of C–C bond between the tubes ranged from 1.38 to 1.55 Å.

The thermodynamic stability of the obtained compounds of CNTs was tested using long molecular dynamic simulation (up to 2 ns) with the increase in the temperature up to 600 K and then up to 1200 K. It was established that the formed covalent bonds of the nanotube framework are conserved under heating by a laser beam even up to 1200 K. In order to verify the obtained results, a fragment of a nanotube framework (including the contact area of the SWCNTs) was studied using a density functional method on the basis of a tight binding scheme (DFTB2).²⁹ The atomic structure of the spliced nanotubes was optimized by the DFTB2 method. The results of the atomic structure investigation confirmed the obtained topology of the contact area of the spliced nanotubes with maintaining the same C–C bonds between the SWCNTs.

Thus, we revealed the decisive factors in the formation of the nanotube framework under the laser heating: (1) the distance between the defective area of the nanotube and the open end of the other nanotubes and (2) the temperature of the laser heating. An increase in temperature up to 80°C to 100°C causes the C–C bonds, because the local heating of the defective areas leads to an increase in amplitude of atomic vibrations and, consequently, to the formation of C–C bonds. A further increase in temperature may slightly increase the number of C–C bonds but also break some bonds, especially in highly strained areas. Thus, in general, high temperatures are not critical for the formation of the nanotube framework.

On the basis of the results of numerical simulation, we established the average time of the direct formation of the bonds between the nanotubes at the distance of 2 to 2.5 Å. This time is 10 to 20 ps, depending on the amount of formed chemical bonds. Figure 4 shows the change in the number of C–C bonds during the formation of a connection between the nanotubes in the case of mixed defects in the SWCNT structure [Fig. 3(a)]. The nature of the adhesion of the nanotubes is clearly observed. It could be seen that two or more bonds can be formed at once, then broken and formed again. However, for a short time all the bonds are stabilized.

3.3 Interaction of Carbon Nanotube Framework with Albumin

The SEM image shows the increase of SWCNTs in diameter from 1.4 to 1.6 nm to 30 to 40 nm [Fig. 2(b)]. This may be

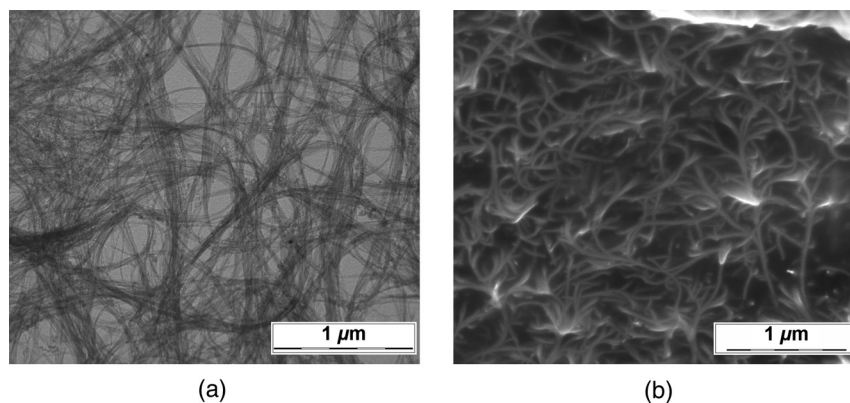


Fig. 2 (a) SEM image of the original SWCNTs on a silicon substrate and (b) image of the transverse cleavage of the composite biostructure.

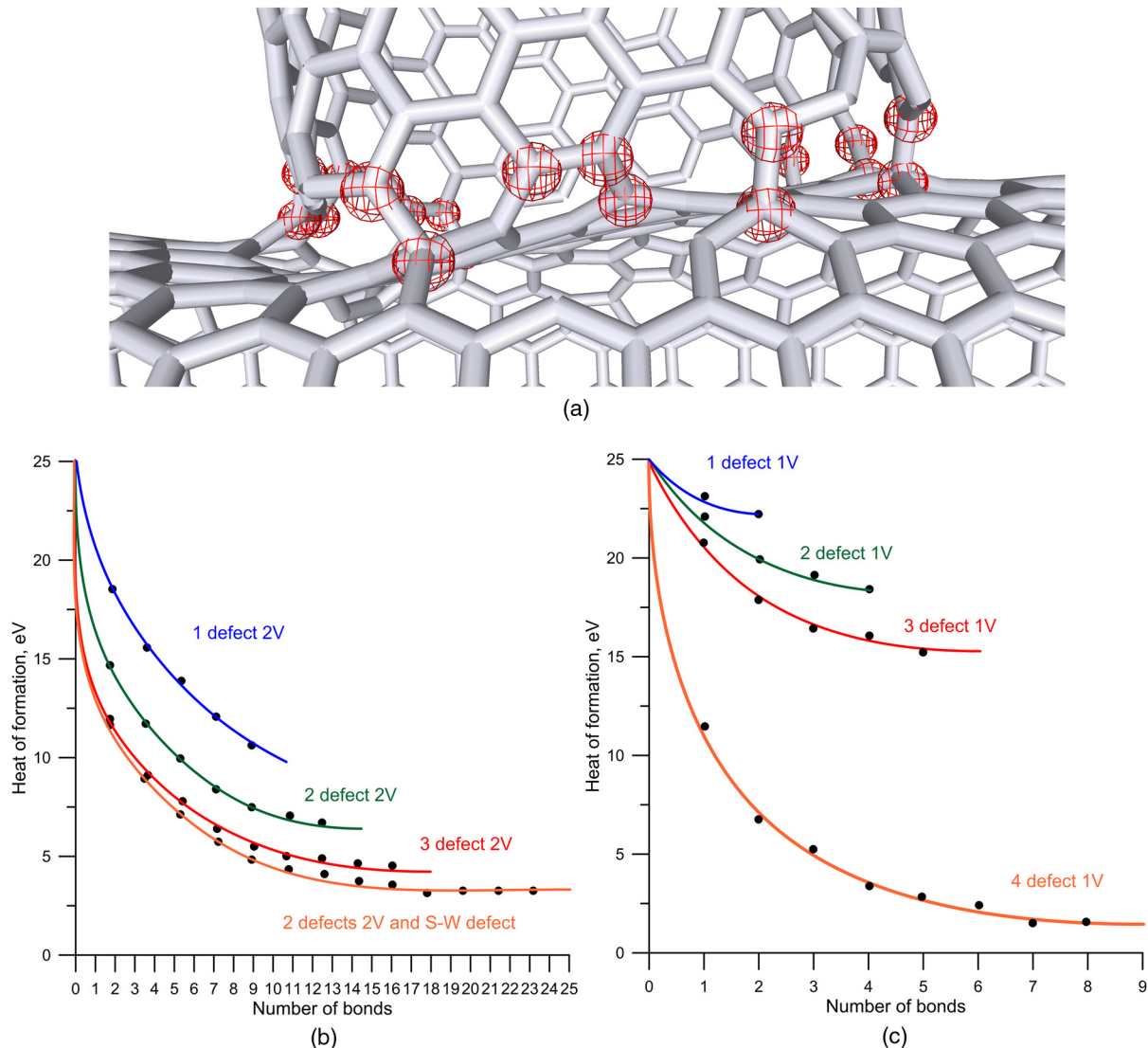


Fig. 3 (a) Simulation of the splicing of the SWCNTs under laser irradiation in the presence of 1V, 2V, and SW defects in nanotubes graphs of the enthalpy of formation of the framework of SWCNTs in the presence of (b) 2V and SW defects and (c) 1V defect.

due to adhesion of SWCNTs in bundles as a result of the van der Waals forces. However, from SEM image of the original SWCNTs, it is possible to notice another kind of the nanotube bundles [Fig. 2(a)]. Another reason for the increase of SWCNTs in diameter is the functionalization of SWCNTs by an albumin layer during the formation of the composite biostructure under the laser heating.

The formation of the composite biostructures in the view of the binding of albumin amino acid residues with the CNTs was described using Raman spectroscopy. The spectrum excited by the neodymium-doped yttrium aluminium garnet (Nd:YAG) laser radiation (wavelength of 1046 nm, power of 0.1 to 0.2 W, depending on the signal/noise ratio) was recorded with a resolution of 4 cm^{-1} , then averaged for over 150 scans, and subjected to inverse Fourier transformation (Fig. 5).

The peaks representing the O-H valence vibrations of water molecules (3283 cm^{-1}) are almost invisible in the spectrum. These peaks are not brightly evident and blurred in the Raman spectroscopy. The peak at 2932 cm^{-1} of valence symmetric vibrations of CH_2 is clearly visible and is characteristic for

all organic compounds. The spectrum presented the peak at 1673 cm^{-1} , amide I (the valence $\text{C}=\text{O}$ vibration), which appears in almost all protein macromolecules. The low intensity for this peak indicates a small fraction of albumin in an alpha-helix conformation. The peak at 1003 cm^{-1} corresponds to the C-C valence vibrations of aromatic organic compounds.

In addition to the deformation vibrations of CH_3 and CH_2 (1443 and 1335 cm^{-1}), we revealed the band characterizing the organic component of the composites at 1593 cm^{-1} in the spectrum of the composite biostructures. This peak corresponds to the valence vibrations (CCH) of the aromatic ring. This spectrum differs from the spectrum of pure albumin by the presence of a chemical bonding with inorganic component of the samples.³⁰ The low intensity of the amides I vibrations, meaning a low proportion of the protein component in an alpha-helix conformation, are due to partial denaturation of albumin under laser exposure during composite creation. It is interesting to note the decrease in peak intensity of the vibration at 1593 cm^{-1} , which is characteristic for CNTs. Apparently, during the obtaining composites, the action of laser radiation and

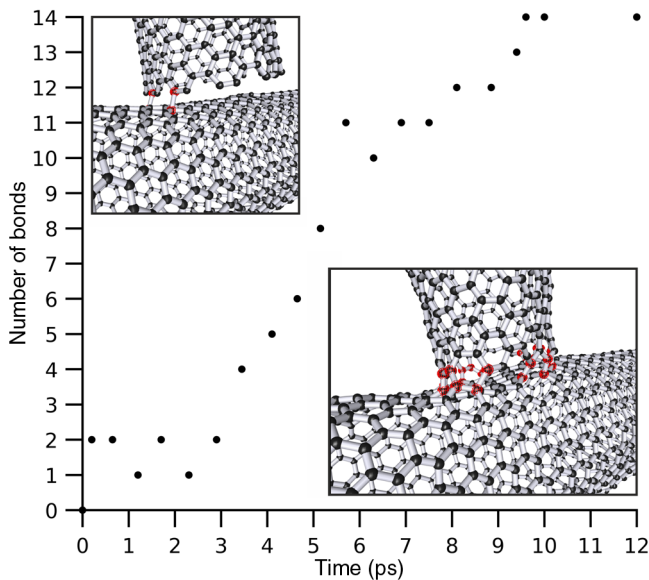


Fig. 4 The change in the number of C—C bonds during the splicing of SWCNTs with few 2V defects and single SW defect.

protein bonding leads to the creation of a material that is different from the structure of pure SWCNTs.

Amino acid residues of Glu and Asp at the surface of the albumin interacting with the SWCNTs were determined from the Raman spectrum of the composite biostructure. The radical of acidic amino acids has an additional carboxyl group, which can form chemical bonds with the surface of the SWCNTs via oxygen atoms. We calculated the interaction energy of an albumin and SWCNTs. These value ranges from 3.7 to 580 kJ/mol. The lower limit of this range corresponds to the van der Waals energies for intermolecular interactions of amino acids in proteins, and the upper one to the energy of covalent bond between CNTs and oxygen amino acid residues of an albumin.³¹

3.4 Atomic Force Microscopy of Composite Biostructure

In order to observe the proliferation of cellular material, we produce flat (as a film) samples of composite biostructure on a silicon substrate [Fig. 1(c)]. The resulting surface topography of composite biostructure (Fig. 6) was obtained using atomic force microscopy (AFM). Figure 6(a) shows the presence of

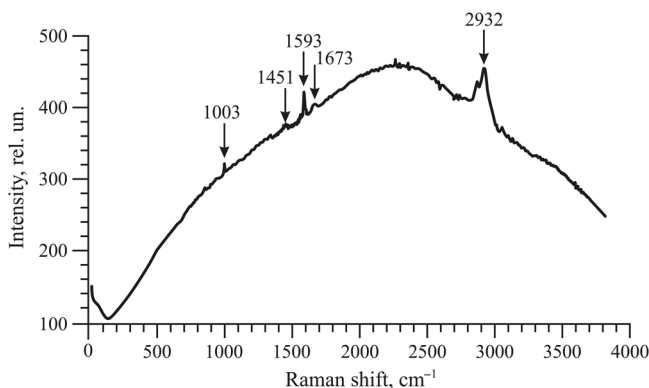


Fig. 5 The Raman spectrum of composite biostructure.

the sections of pores with the size ranging from 30 to 120 nm (dark spots). The type and number of pores depended on the technological parameters of the sample preparation (concentration of SWCNTs, the time and power of laser exposure). The number of pores and their size decreased with increasing concentration in the initial albumin dispersion. This may be due to the reinforcing effect of SWCNTs during the formation of the framework under laser radiation.

3-D AFM images of the composite biostructures based on SWCNTs exhibit low (−12.5 nm) and high (+6.3 nm) sections of the samples [Fig. 6(b)]. The surface structure was uniform with periodically recurring cavities in the form of pores.

3.5 Cell Proliferation on Composite Biostructures

The proliferation of living cells—the fibroblasts on the surface of a composite biostructure—is shown after 3, 24, 48, and 72 h of incubation in CO₂-thermostat using the optical microscopy (Fig. 7). The samples after 3 h of incubation showed a slight tendency to distend with retaining an almost rounded shape. The size of the cells was about 50 μm. The size of the cellular appendages was 10 to 50 μm. After 24 h of incubation, the cells were more flattened on the surface with taking an elongated oblong shape [Fig. 7(a)]. The number of cells that stuck to the sample after 24 h was greater than after 3 h. A greater degree of cell proliferation was observed in the samples incubated for 48 and 72 h. The size of fibroblasts increased, and the cells filled the entire area of the sample.

Microimages have shown that after 72 h, the largest number of cells was observed on the surface of the composite biostructure sample. Their distribution was denser in comparison with the control samples on the basis of a pure albumin film.

In order to study the effect of the composite biostructures on the morphology of fibroblasts, we scanned the samples using AFM [Fig. 7(b)]. For this, the cells on the sample were covered with a composition based on glutaraldehyde for a certain time interval during incubation. After 48 h of incubation, the cells were more flattened on the surface of samples in comparison with the samples after 24 h of incubation. It should be noted that after 48 h the sample surface was almost completely filled with cells. A noticeable accumulation of SWCNTs functionalized by an albumin layer did not have an adverse impact on the cell structure. Over time, the number of arms due to which the fibroblasts well attached to the porous surface composite biostructure increased. After 72 h of incubation, the fibroblasts were more organized and filled all of the available space. Nuclei and nucleoli were clearly visible. A comparison of the morphology of the fibroblasts grown on the samples of the composite biostructures and on the control cover glasses did not allow us to determine what irregularities occurred in the development of the cell. This is because the size and shape of the organelles in the fibroblasts on the composite biostructures did not differ from the structure of the control cells on the cover glasses. Thus, the samples did not exert a toxic effect on the cells and did not change their normal morphology.

4 Discussion

Under laser irradiation of the albumin aqueous solution of SWCNTs in the near-infrared region, an intensive absorption of radiation occurred. This process was accompanied by heating of the nanotubes. As is known, the CNTs have high thermal conductivity and elasticity. This fact allows them to retain structural integrity even under very strong heating and to distribute thermal

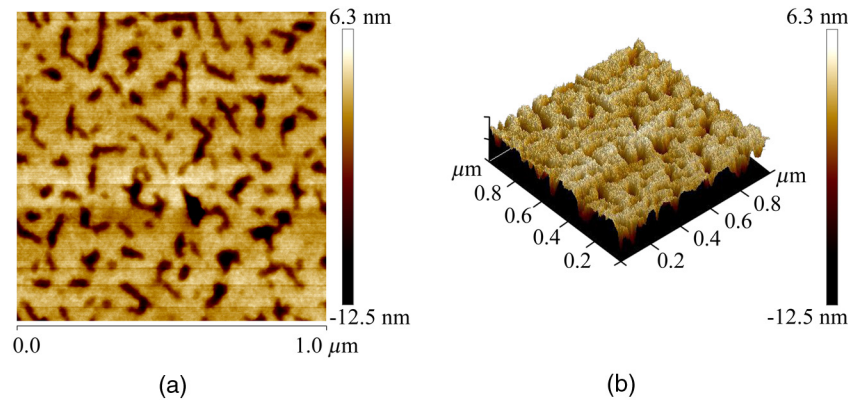


Fig. 6 AFM images of a composite biostructure, (a) two-dimensional view and (b) 3-D view.

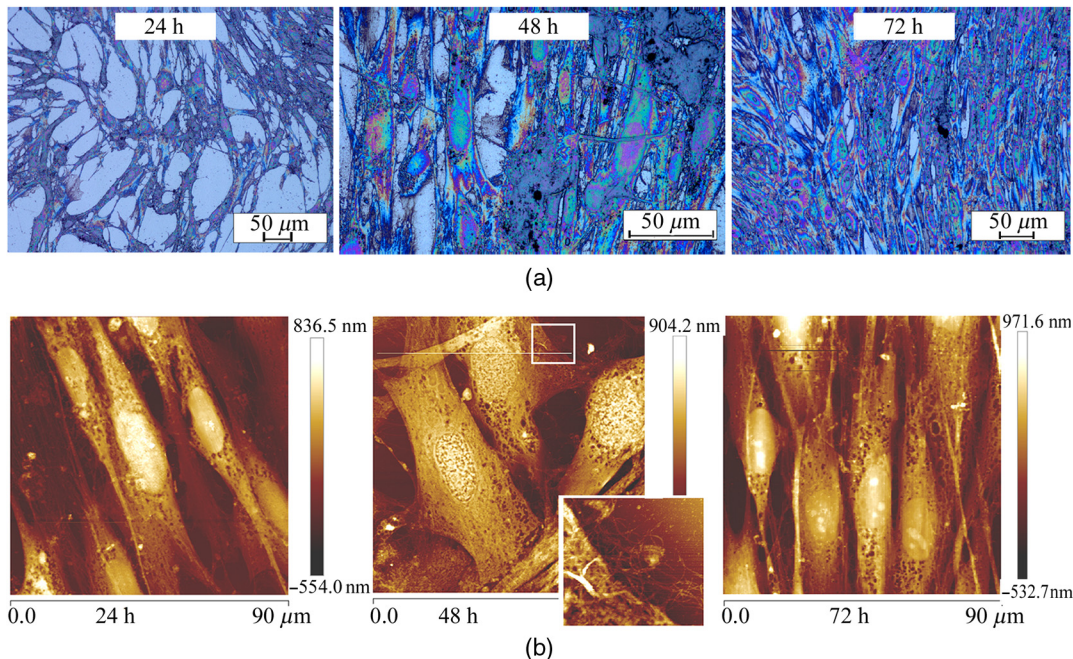


Fig. 7 Images of (a) optical microscopy and (b) AFM fibroblasts after 24, 48, and 72 h of incubation on the surface of the composite biostructures.

energy throughout their length. However, significant heating will occur at the ends of the nanotube and in the areas of the localized defects where the thermal conductivity is markedly reduced. Different kinds of defects are caused in the nanotubes during their synthesis and under heating by laser radiation. The open ends of nanotubes and areas with the defects are the most chemically active. Therefore, we suggested that the SWCNTs will be spliced namely in the defective areas. The numerical simulation showed that the splicing of nanotubes into a framework starts under the laser heating up to a temperature of 353 K. This process occurs within a few nanoseconds. When the temperature increases up to large values, for example, up to 1200 K, the formation of nanotube contacts proceeds faster, namely for 10 to 12 ps. It is important to note that the formed nanotube framework is not destroyed under heating up to 1200 to 1400 K, retaining its thermodynamic stability.

In the composite biostructures, the bonding of SWCNTs with the albumin molecules occurs using the Glu and Asp amino acid

residues. This bond forms between the atoms of CNTs and oxygen atoms of amino acid residues of albumin. The results of molecular dynamic simulation showed that an increase in the number of oxygen atoms leads to a decrease in the interaction energy between SWCNTs and albumin. The addition of the oxygen atoms to the SWCNT leads to a deformation of the nanotube. The more oxygen atoms, the deformation is stronger. The change in the attachment points of oxygen atom to the nanotube oxygen atoms allows us to configure the desired shape of the nanotube framework in the albumin matrix. This in turn will determine the conditions of the cell regeneration for certain biological tissues.

The composite biostructures based on the albumin aqueous solution of SWCNTs have a developed surface with periodic peaks and troughs. It can be seen from the AFM images and is associated with CNT framework, which is formed under laser radiation. This type of surface provides a high degree of adhesion of the fibroblast cells in the samples, as is shown in Ref. 19.

Thus, the colonization and growth of cells are provided on the surface of the composite biostructures over time. This is associated with the better cellular proliferation on the porous surfaces. The fibroblasts have an ordered arrangement on the nanostructured surface of the samples. Within 48 h, the surface of the composite biostructures is filled with the cells almost completely. The AFM images demonstrate the accumulation of CNTs under fibroblasts. This accumulation does not adversely affect on the morphology of the cells.

5 Conclusions

As a result of the investigations, we found out the fundamental possibility of obtaining the composite biostructures by the evaporation of the albumin aqueous solution of SWCNTs using femtosecond laser radiation. By the method of molecular dynamic simulation, we proved the formation of a framework of nanotubes by their splicing at the defective areas under the laser heating. The interaction energy of the nanotube framework with an albumin matrix was determined. The technology for producing the framework by the bonding of oxygen atoms of albumin amino acid residues with the carbon atoms of SWCNTs was presented. The positive impact of the created composite biostructures on the fibroblasts cells was proved. The tissue engineering matrices for the regeneration of connective tissues can be created from the composite biostructures. The proliferation of living cells and the subsequent restoration of 3-D structure of the biotissues will be provided during the implantation of the composite biostructure into pathologically altered areas of connective tissue (e.g., cavities of the epithelium, cartilage, etc.).

Disclosures

The authors have no financial interests in the manuscript and no conflicts of interest to disclose.

Acknowledgments

This work was provided by the Ministry of Education and Science of the Russian Federation (Agreement 14.578.21.0221 RFMEFI57816X0221). The authors thank M. Mezentseva and I. Suetina from Tissue Culture Laboratory of Federal Research Center N.F.Gamaley of Epidemiology and Microbiology (Russia, Moscow) for help while working with living cells. The authors also thank L. Ichkitidze, PhD, M. Savelyev, PhD, and Professor S. Selishchev for their recommendations that assisted the research.

References

1. P. Bajaj et al., "3D biofabrication strategies for tissue engineering and regenerative medicine," *Annu. Rev. Biomed. Eng.* **16**, 247–276 (2014).
2. S. V. Murphy and A. Atala, "3D bioprinting of tissues and organs," *Nat. Biotechnol.* **32**(8), 773–785 (2014).
3. F. Guillemot et al., "High-throughput laser printing of cells and biomaterials for tissue engineering," *Acta Biomater.* **6**(7), 2494–2500 (2010).
4. S. K. Seidlits, C. E. Schmidt, and J. B. Shear, "High-resolution patterning of hydrogels in three dimensions using direct-write photofabrication for cell guidance," *Adv. Funct. Mater.* **19**(22), 3543–3551 (2009).
5. F. Melchels, J. Feijen, and D. Grijpma, "A review on stereolithography and its applications in biomedical engineering," *Biomaterials* **31**(24), 6121–6130 (2010).
6. M. Farsari, G. Filippidis, and T. S. Drakakis, "Three-dimensional biomolecule patterning," *Appl. Surf. Sci.* **253**(19), 8115–8118 (2007).
7. W. Bian, D. Li, and Q. Lian, "Fabrication of a bio-inspired beta-tricalcium phosphate/collagen scaffold based on ceramic stereolithography

and gel casting for osteochondral tissue engineering," *Rapid Prototyping J.* **18**(1), 68–80 (2012).

8. B. Duan et al., "Three-dimensional nanocomposite scaffolds fabricated via selective laser sintering for bone tissue engineering," *Acta Biomater.* **6**(12), 4495–4505 (2010).
9. S. F. S. Shirazi et al., "A review on powder-based additive manufacturing for tissue engineering: selective laser sintering and inkjet 3D printing," *Sci. Technol. Adv. Mater.* **16**(3), 033502 (2015).
10. T. R. Northen, D. C. Brune, and N. W. Woodbury, "Synthesis and characterization of peptide grafted porous polymer microstructures," *Biomacromolecules* **7**(3), 750–754 (2006).
11. P. Danilevicius et al., "Micro-structured polymer scaffolds fabricated by direct laser writing for tissue engineering," *J. Biomed. Opt.* **17**(8), 081405 (2012).
12. S. Engelhardt et al., "Fabrication of 2D protein microstructures and 3D polymer-protein hybrid microstructures by two-photon polymerization," *Biofabrication* **3**(2), 025003 (2011).
13. A. Selimis, V. Mironov, and M. Farsari, "Fabrication of microscale medical devices by two-photon polymerization with multiple foci via a spatial light modulator," *Biomed. Opt. Exp.* **2**(11), 3167–3168 (2011).
14. S. D. Gittard, A. Nguyen, and K. Obata, "Direct laser writing: principles and materials for scaffold 3D printing," *Microelectron. Eng.* **132**, 83–89 (2015).
15. D. Simhon et al., "Temperature-controlled laser-soldering system and its clinical application for bonding skin incisions," *J. Biomed. Opt.* **20**(12), 128002 (2015).
16. C. B. Bleustein, D. Felsen, and D. P. Poppas, "Welding characteristics of different albumin species with and without fatty acids," *Lasers Surg. Med.* **27**(2), 82–86 (2000).
17. A. Bujacz, "Structures of bovine, equine and leporine serum albumin," *Acta Crystallogr.* **D68**, 1278–1289 (2012).
18. A. Y. Gerasimenko et al., "Biomedical applications of promising nanomaterials with carbon nanotubes," *Biomed. Eng.* **48**(6), 310–314 (2015).
19. L. P. Zanello et al., "Bone cell proliferation on carbon nanotubes," *Nano Lett.* **6**(3), 562–567 (2006).
20. E. Hirata et al., "3D collagen scaffolds coated with multiwalled carbon nanotubes: initial cell attachment to internal surface," *J. Biomed. Mater. Res. Part B Appl. Biomater.* **93B**(2), 544–550 (2010).
21. A. Y. Gerasimenko et al., "Research on limiting of high power laser radiation in nonlinear nanomaterials," *Proc. SPIE* **9237**, 923712 (2014).
22. A. Y. Gerasimenko et al., "Laser nanostructuring 3D bioconstruction based on carbon nanotubes in a water matrix of albumin," *Proc. SPIE* **9887**, 988725 (2016).
23. J. Che, T. Cagin, and W. A. Goddard, "Thermal conductivity of carbon nanotubes," *Nanotechnology* **11**, 65–69 (2000).
24. H. F. Bettinger, "The reactivity of defects at the sidewalls of single-walled carbon nanotubes: the Stone–Wales defect," *J. Phys. Chem. B* **109**(15), 6922–6924 (2005).
25. The Kvazar, <http://nanokvazar.ru> (10 January 2017).
26. D. W. Brenner, O. A. Shenderova, and J. A. Harrison, "A second-generation reactive empirical bond order (REBO) potential energy expression for hydrocarbons," *J. Phys. Condens. Matter* **14**(4), 783–802 (2002).
27. O. E. Glukhova and M. M. Slepchenkov, "Electronic properties of the functionalized porous glass-like carbon," *J. Phys. Chem. C* **120**(31), 17753 (2016).
28. V. V. Shunaev and O. E. Glukhova, "Topology Influence on the process of graphene functionalization by epoxy and hydroxyl groups," *J. Phys. Chem. C* **120**(7), 4145–4149 (2016).
29. M. Elstner et al., "Self-consistent-charge density-functional tight-binding method for simulations of complex materials properties," *Phys. Rev. B* **58**(11), 7260–7268 (1998).
30. I. I. Bobrinetsky et al., "Spectral characteristics of materials based on carbon nanotubes," *Biomed. Eng.* **48**(6), 318–323 (2015).
31. G. N. Ten et al., "Calculation and analysis of the structure and vibrational spectra of uracil tautomers," *J. Struct. Chem.* **51**(1), 32–39 (2010).

Alexander Yu. Gerasimenko is an associated professor at the National Research University of Electronic Technology. He received his PhD in condensed-matter physics from the National Research University of Electronic Technology in 2010. He is the author of more than 40 journal papers and has written five book chapters.

His current research interests include nonlinear optics, interaction of radiation with nanomaterials, and optoelectronic biomedical systems. He is a member of SPIE and advisor of the student chapter of SPIE.

Olga E. Glukhova, Doctor of Science in physics and mathematics, is a head of the Department of Radiotechnique and electrodynamics at Saratov State University and leads the Division of Mathematical Modeling in Educational and Scientific Institution of Nanostructures and Biosystems at Saratov State University. Her main fields of investigation are nanoelectronics, molecular modeling of biomaterials and nanostructures, mechanics of nanostructures, molecular dynamics, and carbon nanostructures. She has published about 170 peer-reviewed journal papers and four monographs.

Georgy V. Savostyanov is an assistant at the Department of Radiotechnique and Electrodynamic at Saratov State University and

a programmer at the Mathematical Modeling in Educational and Scientific Institution of Nanostructures and Biosystems at Saratov State University. He is a member of the Glukhova Research Group (nankovazar.ru). He has a diploma of higher education in a specialty, applied mathematics and computer science. His research interests are nanoelectronics, nanostructures, molecular modeling, programming, and high performance computing. He has 17 published works.

Vitaly M. Podgaetsky, Doctor of Science in physics and mathematics, is a professor at the National Research University of Electronic Technology. His main fields of investigation are laser pumping lamps, cooling liquids, and laser systems for nanomedicine. He has published over 220 peer-reviewed journal papers and 60 inventions.